scientific reports

Check for updates

OPEN

MiR-556-3p mediated repression of klotho under oxidative stress promotes fibrosis of renal tubular epithelial cells

Dong Zhang[1]✉, Zongying Li[1], Yuan Gao[1] & Hailing Sun[2]

Chronic kidney disease (CKD) is a global health issue characterized by renal fibrosis, which leads to irreversible tissue damage. Oxidative stress plays a key role in driving the fibrotic processes associated with CKD. This study investigates the roles of oxidative stress, miR-556-3p, and klotho in renal tubular epithelial cells, focusing on their influence on fibrotic pathways. Using human renal tubular epithelial cells HK-2, we conducted various in vitro assays to measure reactive oxygen species (ROS) levels, cell death, viability, and proliferation. Oxidative stress, induced by H_2O_2 treatment, was found to suppress klotho expression while increasing the expression of fibrotic markers. Overexpression of klotho mitigated these effects, highlighting its protective role against oxidative stress-induced fibrosis. Moreover, miR-556-3p was upregulated in response to oxidative stress activated transcription factor Nuclear Factor Erythroid 2-Related Factor 2 (Nrf2), contributing to the suppression of klotho. Inhibition of Nrf2, a key regulator of oxidative stress responses, attenuated the expression of miR-556-3p and fibrotic markers. Targeting the Nrf2-miR-556-3p-klotho axis may offer novel therapeutic avenues to restore klotho levels and attenuate renal fibrosis. Our study contributes significantly to the understanding of the molecular mechanisms driving CKD progression and highlights potential targets for future pharmacological intervention.

Keywords Chronic kidney disease, Oxidative stress, Klotho, miR-556-3p, Nrf2, Renal fibrosis

Chronic Kidney Disease (CKD) is a significant global health issue, affecting over 800 million individuals worldwide, with a prevalence ranging from 10.5 to 13.1%. CKD is more common in older individuals, women, racial minorities, and those with diabetes and hypertension. The incidence and prevalence of CKD have been increasing over the years, with a notable rise in mortality rates, making CKD one of the leading causes of death globally. Understanding the pathogenesis of CKD is crucial for implementing effective prevention and treatment strategies[1–5].

CKD is characterized by renal fibrosis, a crucial factor leading to irreversible tissue damage and functional decline in the kidneys. Fibrosis in CKD involves the progressive accumulation of fibrous collagens, loss of capillary networks, and activation of myofibroblasts[6]. Oxidative stress plays a pivotal role in kidney damage by promoting fibrotic processes through various mechanisms. Studies have shown that oxidative stress leads to the overproduction of ROS, triggering sustained cell growth, inflammation, and excessive tissue remodeling, ultimately accelerating renal damage[7,8]. This imbalance between ROS generation and detoxification alters cellular macromolecules, leading to organ dysfunction, particularly in CKD[9]. Additionally, profibrogenic agonists like Angiotensin II and platelet-derived growth factor upregulate the expression of protein deglycase DJ-1, a crucial ROS scavenger, in renal cells[7,10].

Klotho, a protein known for its anti-aging properties, plays a crucial role in renal physiology by exerting protective effects on kidney function. Research indicates that soluble klotho levels decrease in conditions like diabetic nephropathy[11], contrast-induced nephropathy[12], and kidney disease. Studies have shown that klotho protects chromosomal DNA from damage, enhances cell survival rates after DNA damage, and regulates pathways related to inflammation, oxidative stress, fibrosis, and metabolism[13]. The decline of klotho expression in CKD has been extensively studied due to its significant implications for disease progression and patient outcomes. Several studies have highlighted the association between reduced klotho levels and increased oxidative stress,

[1]The First Department of Nephrology, Cangzhou Central Hospital, 16 West Xinhua Road, Cangzhou 061000, Hebei, China. [2]Department of Hematology, Cangzhou Central Hospital, Cangzhou 061000, Hebei, China. ✉email: blacksisyphus@126.com

inflammation, and fibrosis in CKD patients. For instance, Jena et al. demonstrated that serum klotho levels negatively correlate with glomerular filtration rate and oxidative stress[14].

In recent years, miRNAs have emerged as critical regulators of gene expression in various pathophysiological processes, including renal fibrosis[15]. Among these, hsa-miR-556 has been identified as a potentially significant player. The levels of miR-556-3p and miR-556-5p derived from hsa-miR-556 were associated renal recovery from severe acute kidney disease[16]. Circulating miR-556-5p has also been associated with kidney damage in Patients with Systemic Lupus Erythematosus[17]. Previous study suggested that klotho is a target of miR-556-3p[18], however, the expression and potential role of miR-556-3p in CKD remains unexplored.

This study elucidates the complex interplay between oxidative stress and klotho in the pathogenesis of renal fibrosis. Understanding these molecular mechanisms can provide valuable insights into the progression of CKD and highlight potential therapeutic targets. Specifically, modulating the Nrf2-miR-556-3p-klotho axis could offer novel interventions to restore klotho levels and attenuate renal fibrosis. This research not only deepens our understanding of CKD pathology but also opens avenues for innovative treatments that could potentially reverse or halt the disease progression.

Cell culture and treatment

Human proximal tubular cells (HK-2 cells) were purchased from the American Tissue Culture Collection (#CRL-2190, Manassas, VA, USA) and maintained in DMEM/F12 (#11320033, Gibco, USA) medium supplemented with 10% fetal bovine serum (#A5256801, GIBCO, USA) and 1% penicillin-streptomycin solution (#15140122, GIBCO, USA), cultured at 37 °C in a humidified 5% CO_2 atmosphere. The cells were seeded in six-well plates and allowed to adhere for 24 h before the addition of indicated concentration of H_2O_2 (0.1, 0.2, 0.5, or 1 mM) for 24 h. For all experiments, each condition was replicated in at least three independent experiments to ensure reproducibility.

EdU ASSAY

To perform an EdU assay (#C0071S, Beyotime, China) on HK-2 cells, cells were seeded in a culture dish and incubated overnight. The next day, the culture medium was replaced with medium containing diluted EdU reagent, and incubated for 24 h for EdU incorporation. The cells were then washed with phosphate-buffered saline (PBS) and fixed with 4% paraformaldehyde (#P0099, Beyotime, China) for 15 min at room temperature. After fixation, cells were permeabilized with 0.5% Triton X-100 (#ST1723, Beyotime, China) for 15 min, followed by the application of a click reaction mixture and incubated for 30 min protected from light. Subsequently, the cells were washed and the nuclei were stained using 1 μg/mL DAPI (#C1002, Beyotime, China) for 10 min. Finally, the cells were washed again and subjected to fluorescence microscopy imaging. The intensity of staining was analyzed using ImageJ software (NIH, USA) to assess the level of ROS, and the data were normalized to the control group.

Nucleus-cytosol fractionation

HK-2 Cells were first suspended in an ice-cold hypotonic buffer comprising 10 mM KCl (#A610440, Sangon Biotech, China), 10 mM HEPES (#ST2425, Beyotime, China) (pH 7.4), 10 mM NaCl (#A610476, Sangon Biotech, China), 0.1 mM EDTA (#B540625, Sangon Biotech, China), 1 mM dithiothreitol (DTT, #A620058, Sangon Biotech, China), and 0.5 mM phenylmethylsulfonyl fluoride (PMSF, #A610425, Sangon Biotech, China). This suspension was incubated on ice for 15 min. Afterwards, 0.6% NP-40 (#A600385, Sangon Biotech, China) was added and the mixture was vortexed briefly for 10 s. The lysates were then centrifuged at 12,000 rpm for 1 min to eliminate nuclei and cell debris. The resulting supernatant, which contains the cytosolic fraction, was collected and subjected to further centrifugation at 12,000 rpm for 30 min at 4 °C. The pellet obtained was resuspended in hypotonic buffer with 0.6% NP-40, vortexed, and washed three times, each time centrifuging at 12,000 rpm for 2 min at 4 °C. Finally, this pellet was resuspended in a buffer with 0.4 M NaCl, 20 mM HEPES (pH 7.4), 1 mM EDTA, 1 mM DTT, and 1 mM PMSF, and incubated on ice for 30 min. After centrifugation at 12,000 rpm for 30 min, the supernatant containing the nuclear fraction was collected. Three independent experiments were performed to ensure reproducibility.

ROS assay

The intracellular ROS levels in HK-2 cells were measured using the dichloro-dihydro-fluorescein diacetate (DCFH-DA, #S0035S, Beyotime, China) assay. Following treatment, HK-2 cells were incubated with DCFH-DA (5 μM) for 30 min at 37 °C in darkness. The fluorescence associated with ROS was then quantified using a fluorescence spectrophotometer (Thermo Fisher Scientific, USA) at excitation and emission wavelengths of 488 nm and 525 nm, respectively. Results were expressed as relative intensity normalized to the control group. Each experimental condition was tested across three biological replicates and at least three independent experiments were conducted.

Cell counting kit-8 (CCK-8) assay

HK-2 cells were plated at a density of 5000 cells per well in 96-well plates. Cell proliferation was measured using the CCK-8 assay kit (#C0038, Beyotime, China). After stimulating the cells, CCK-8 solution was introduced to the wells, and the plates were incubated for 1 h at 37 °C in a humidified atmosphere consisting of 95% air and 5% CO_2. Absorbance readings were taken at 450 nm using a Microplate Reader (Bio-Rad, USA). Each experimental condition was tested across three biological replicates and at least three independent experiments were conducted.

Western blotting

Proteins for Western blot analysis were extracted using RIPA lysis buffer (#P0013B, Beyotime, China), supplemented with cOmplete protease inhibitors (#04693132001, Roche, Switzerland) and PhosSTOP (#4906845001, Roche, Switzerland). Protein concentrations were determined using the BCA™ Protein Assay Kit (#A55864, Pierce, USA). The Western blotting was performed on a Bio-Rad Bis-Tris Gel system following the instructions provided by the manufacturer. Primary antibodies were diluted in 5% blocking buffer and incubated with the membranes overnight at 4 °C. After washing, membranes were incubated with horseradish peroxidase (HRP)-conjugated secondary antibodies for 1 h at room temperature. Following another rinse, the blots and antibodies were processed in the Bio-Rad ChemiDoc™ XRS system. Subsequently, 200 µl of Immobilon Western Chemiluminescent HRP Substrate (#WBKLS0050, Millipore, USA) was applied to the membrane surfaces. Signal detection and band intensity analysis were carried out using Image Lab™ Software (Bio-Rad, USA). Three independent experiments were performed to ensure reproducibility. The following primary antibodies were used: klotho (#ab181373, 1:1000 dilution, Abcam, UK), COL1A1 (#C2456, 1:1000 dilution, Sigma-Aldrich, USA), Glyceraldehyde 3-phosphate dehydrogenase (GAPDH) (#MAB374, 1:5000, Millipore, USA), COL3A1 (#30565, 1:1000 dilution, Cell Signaling Technology, USA), fibronectin (#26836, 1:1000 dilution, Cell Signaling Technology, USA), αSMA (#ab5694, 1:2000 dilution, Abcam, UK), Nrf2 (#sc-365949, 1:500 dilution, Santa Cruz Biotechnology, USA), and CTGF (#sc-365970, 1:500 dilution, Santa Cruz Biotechnology, USA). Results were quantified by densitometry using ImageJ software and expressed as the ratio of the target protein to GAPDH, providing normalized data that facilitates comparison across samples.

miRNAs transfection

The scramble miRNA mimic negative control (#HY-R04602, MedChemExpress, USA), has-miR-556-3p mimic (#HY-R01719, MedChemExpress, USA), miRNA inhibitor negative control (#HY-RI04602, MedChemExpress, USA), and miR-556-3p inhibitor (#HY-RI01719, MedChemExpress, USA)) purchased from MedChemExpress. Transfections into cells were carried out utilizing Lipofectamine 3000 reagent (#L3000008, Invitrogen, USA), strictly adhering to the provided protocol.

Quantitative reverse transcription polymerase chain reaction (RT-qPCR)

Total RNA from cultured cells was isolated using the RNA pure Rapid Extraction Kit (#RP1202, Bioteke Corporation, China), following the manufacturer's protocol. For miRNA reverse transcription, cDNA synthesis was performed by appending a poly (A) tail to the 3′ end of miRNAs using an oligo (dT) adaptor primer and Super M-MLV reverse transcriptase (#PR6502, Bioteke Corporation, China). For mRNA, reverse transcription utilized a mix containing random primers and M-MLV reverse transcriptase. The resulting cDNA was then amplified through RT-qPCR employing SYBR green Master Mix on an Exicycler 96 Real-Time Quantitative Thermal Block (BIONEER, South Korea). U6 served as the internal standard for miRNA expression, and GAPDH for mRNA expression levels. Specific primers U6 snRNA (TACCTTGCGAAGTGCTTAAAC) and miRNA-556-3p (GTCGTATCCAGTGCGTGTCGTGGAGTCGGCAATTGCACTGGATACGACAAAGA) were used to synthesize the cDNA of U6 and miR-556-3p, respectively[19]. RT-qPCR conditions included an initial incubation at 95 °C for 10 min, followed by 40 cycles of 95 °C for 10 s, 60 °C for 20 s, and 72 °C for 30 s, with a final 5-minute incubation at 4 °C. Relative expression was quantified using the $2^{-\Delta\Delta CT}$ method, with each sample analyzed in triplicate across three independent experiments. Primers were synthesized by Sangon Biotech (China) and the sequences were listed below:

miRNA-556-3p forward: 5′-ATATTACCATTAGCTCATCTTT-3′,
miRNA-556-3p reverse: 5′-GTCGTATCCAGTGCGTGTCGTG-3′;
U6 forward: 5′-GTGCTCGCTTCGGCAGCACAT-3';
U6 reverse: 5′-TACCTTGCGAAGTGCTTAAAC-3′;
Nrf2 forward: 5'-TCAGCGACGGAAAGAGTATGA-3';
Nrf2 reverse: 5'-CCACTGGTTTCTGACTGGATGT-3';
Fibronectin forward: 5'-CGGTGGCTGTCAGTCAAAG-3';
Fibronectin reverse: 5'-AAACCTCGGCTTCCTCCATAA-3';
αSMA forward: 5'-AAAAGACAGCTACGTGGGTGA-3';
αSMA reverse: 5'-GCCATGTTCTATCGGGTACTTC-3';
COL1A1 forward: 5'-GAGGGCCAAGACGAAGACATC-3';
COL1A1 reverse: 5'-CAGATCACGTCATCGCACAAC-3';
COL3A1 forward: 5'-GGAGCTGGCTACTTCTCGC-3';
COL3A1 reverse: 5'-GGGAACATCCTCCTTCAACAG-3';
Klotho forward: 5'-GTGCGTCCATCTGGGATACG-3';
Klotho reverse: 5'-TGTCGCGGAAGACGTTGTT-3';
CTGF forward: 5'- CAGCATGGACGTTCGTCTG-3';
CTGF reverse: 5'-AACCACGGTTTGGTCCTTGG-3'.

Terminal deoxynucleotidyl transferase dUTP nick end labeling (TUNEL) assay

To conduct a TUNEL assay (#C1086, Beyotime, China) on HK-2 cells, HK-2 cells were seeded in a culture dish and incubated overnight. After the desired treatment, Medium was removed and the cells were washed with PBS. The cells were fixed with 4% paraformaldehyde for 15 min at room temperature. followed by wash of the cells again with PBS and permeabilization with 0.1% Triton X-100 in 0.1% sodium citrate for 5 min on ice. The TUNEL reaction mixture was added to the cells and incubated in a dark, humidified environment at 37 °C for 1 h. After incubation, the cells were rinsed with PBS to remove any unbound TUNEL reagent. The images were

analyzed to assess the proportion of TUNEL-positive cells, which reflects the extent of apoptosis in the cell population. Three independent experiments were performed to ensure reproducibility.

Statistical analysis

All experiments were conducted in triplicate. Statistical evaluations were carried out using GraphPad Prism version 6.0. Prior to conducting the analysis, the assumptions of ANOVA, including normal distribution and homogeneity of variances, were verified using Shapiro-Wilk and Levene's tests, respectively. Data were analyzed using one-way ANOVA to determine the significant differences among treatment groups. To further explore these differences, post-hoc pairwise comparisons were conducted using the Tukey's Honest Significant Difference (HSD) test when equal variances were assumed, and the Bonferroni correction was applied in cases of multiple comparisons to control the type I error rate. Results are presented as mean ± standard deviation (SD), and a p-value of < 0.05 was considered statistically significant. All experiments were conducted with a minimum of $n = 3$ biological replicates per treatment group to ensure adequate statistical power.

Result

Oxidative stress suppresses the expression of klotho

Previous study reported that the expression of klotho is regulated by oxidative stress[20]. After treating human renal tubular epithelial cells (HK-2) with increasing concentrations of H_2O_2 (oxidant) for 24 h, gradual increasing of ROS levels, concomitant increasing of cells death, and decreasing of cell viability was observed (Fig. 1A and C). In addition, cell proliferation was also suppressed (Fig. 1D). Treatment with H_2O_2 resulted in a progressive decline in both mRNA and protein levels of klotho (Fig. 1E and F). Additionally, markers associated with fibrosis, such as COL1A1 (Collagen, type I, alpha 1), COL3A1, fibronectin, and alpha smooth muscle actin (α-SMA), were found to increase correspondingly (Fig. 1E and F). These findings underscore the inhibitory role of oxidative stress on klotho expression, which may contribute to the pathogenesis of renal fibrosis in chronic kidney disease.

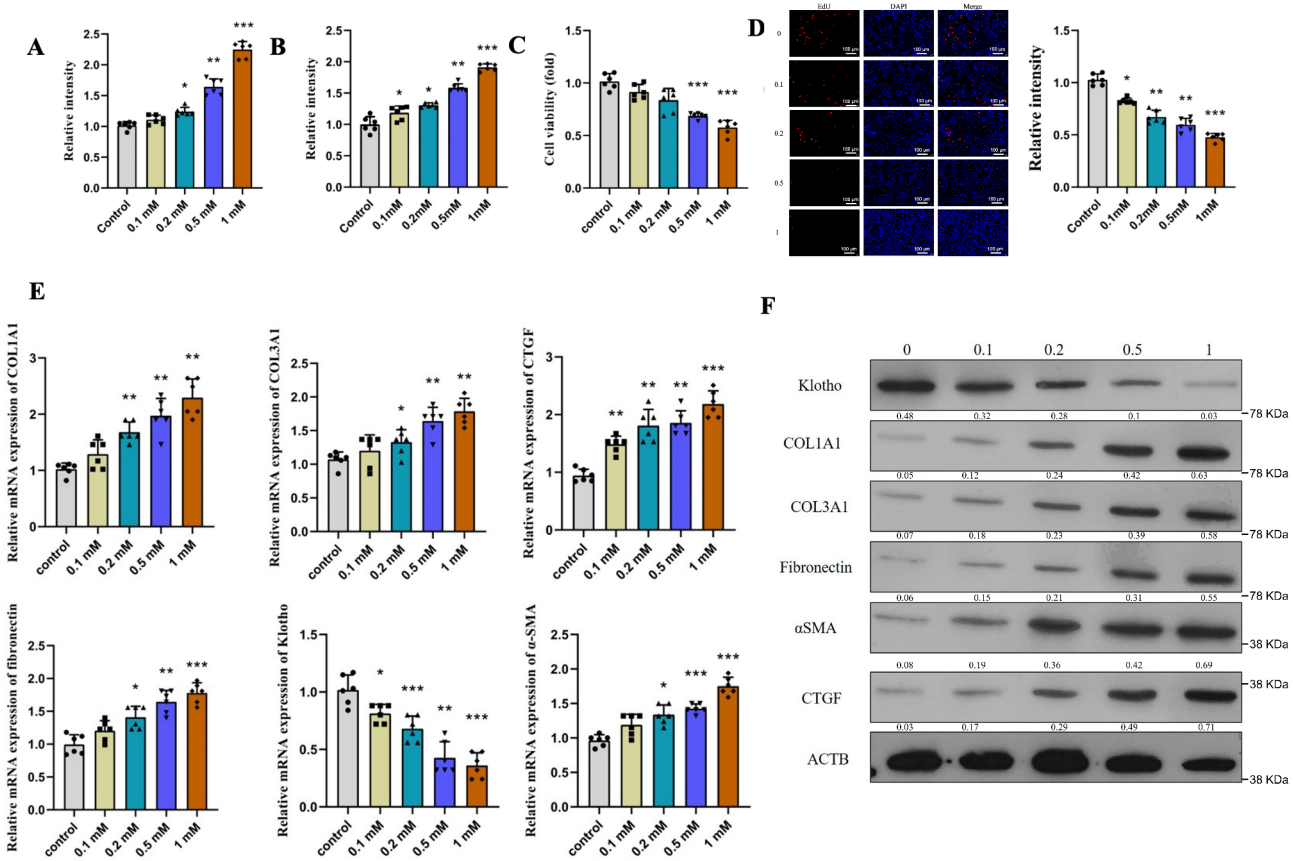

Fig. 1. Oxidative stress suppresses the expression of Klotho. (**A**–**C**) ROS levels (**A**), cell apoptosis (**B**), cell viability (**C**), and cell proliferation (**D**) in HK-2 cells stimulated by indicated concentration of H_2O_2. (**E**) mRNA levels of fibrosis-related genes in HK-2 cells challenged with indicated concentration of H_2O_2. (**F**) protein levels of fibrosis-related genes in HK-2 cells stimulated by indicated concentration of H_2O_2. $^*p < 0.05$, $^{**}p < 0.01$, $^{***}p < 0.001$, $^{***}p < 0.0001$.

ROS scavenger upregulates Klotho and inhibits the expression of fibrosis-related genes

In cells treated with H_2O_2 alone, there was a marked decrease in klotho expression, concurrent with increased expression of fibrosis-associated genes such as COL1A1, COL3A1, fibronectin, and α-SMA. However, when ROS scavenger N-acetyl-l-cysteine (NAC) was added to the H_2O_2-treated cells, ROS levels were significantly reduced (Fig. 2A), along with a partial restoration of klotho expression and a significant reduction in the levels of the fibrosis-related genes (Fig. 2B and C). This reversal suggests that by scavenging ROS, NAC mitigates the oxidative stress-induced suppression of klotho and concurrently inhibits the progression of fibrosis in the renal tubular epithelial cells.

Klotho inhibits the expression of fibrotic genes in HK-2 cells

To interrogate the role of klotho in modulating oxidative stress-mediated fibrosis in HK-2 cell, klotho was overexpressed (Fig. 3A). Overexpression of klotho significantly affected cellular response to oxidative stress. Overexpression of klotho repressed H_2O_2 induced ROS production (Fig. 3B), reduced cell death (Fig. 3C), increased cell viability (Fig. 3D) and proliferation (Fig. 3E). In the control group (Vector CTRL), treatment with H_2O_2 led to a marked increase in the expression of fibrosis-related genes such as COL1A1, COL3A1, fibronectin, and α-SMA (Fig. 3F and G). Conversely, in the Klotho-OE group, there was a corresponding decrease in the expression of the fibrosis-associated genes after H_2O_2 treatment (Fig. 3F and G). The enhanced expression of klotho appeared to confer a protective effect against the induction of fibrotic gene expression under oxidative stress conditions.

ROS inhibits klotho expression by upregulating miR-556-3p

Previous study indicated that the expression of klotho was regulated by miR-556[21], but it remains to be determined if oxidative stress control klotho expression through miR-556. We observed a significant increase of miR-556 after H_2O_2 treatment (Fig. 4A), while treatment with NAC decreased miR-556 expression (Fig. 4B). To investigate if miR-556 regulate klotho expression in HK-2 cell, we treated the cells with miR-556 mimic, the expression of klotho was reduced, while fibrotic genes were upregulated (Fig. 4C and D). Consistently, miR-556

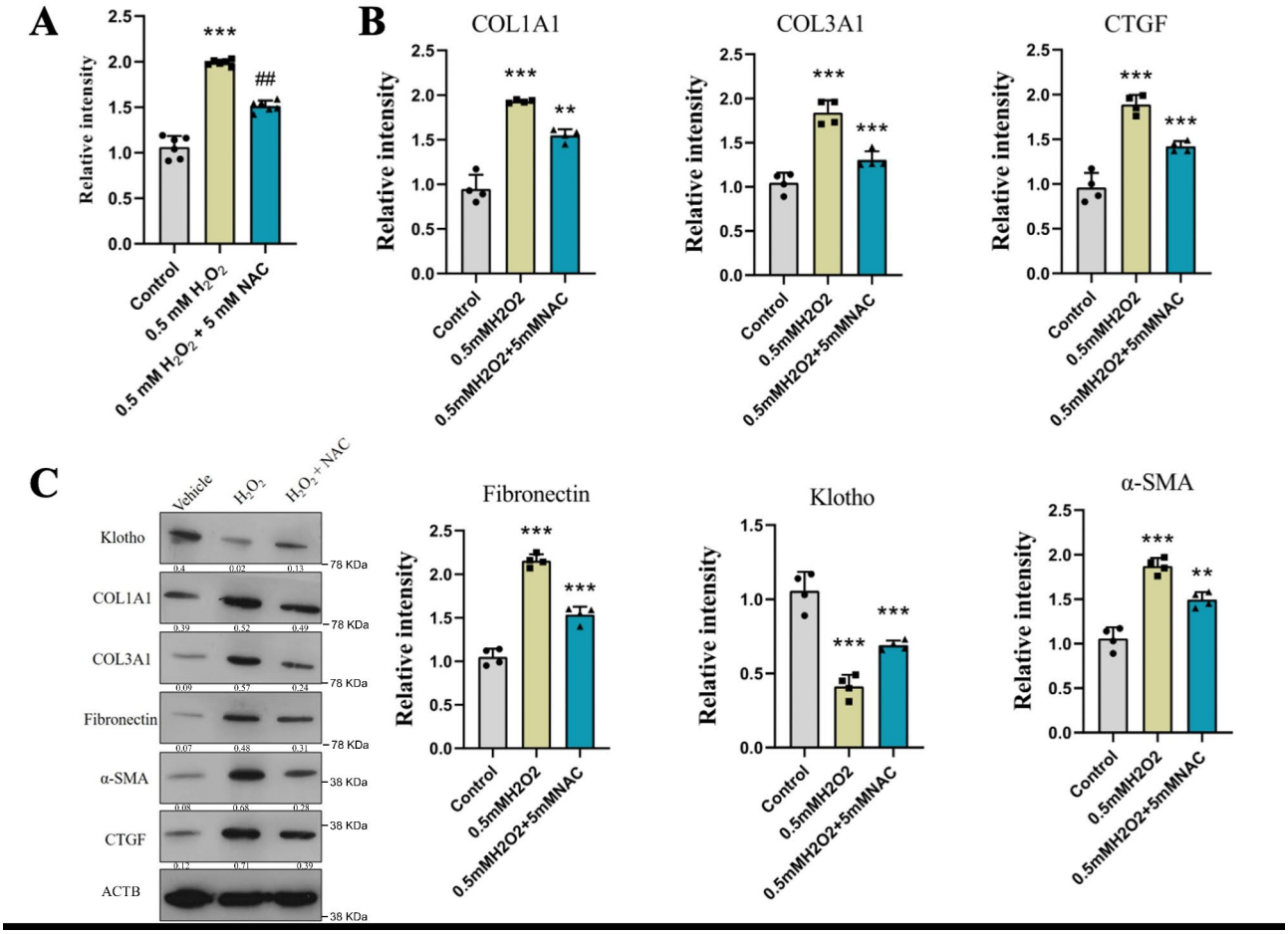

Fig. 2. ROS scavenger upregulates Klotho and inhibits the expression of fibrosis-related genes. (**A**) ROS levels in HK-2 cells challenged with H_2O_2 and ROS scavenger NAC. (**B**–**C**) mRNA (**B**) and protein (**C**) levels of klotho and fibrosis-related genes in HK-2 cells stimulated with H_2O_2 and ROS scavenger NAC. $^{**}p < 0.01$, $^{***}p < 0.001$, $^{\#\#}p > 0.05$.

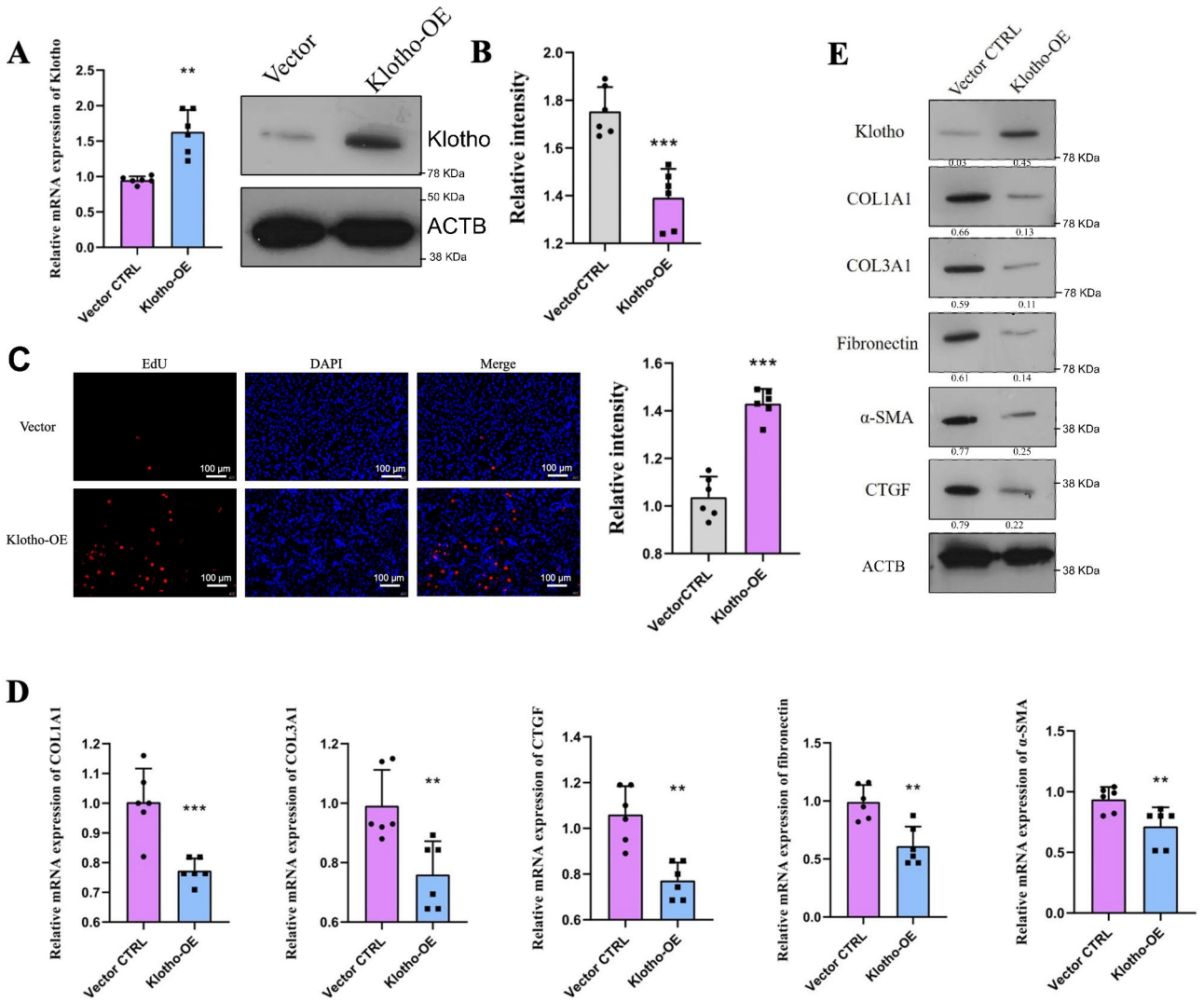

Fig. 3. Klotho inhibits the expression of fibrotic genes in HK-2 cells. Klotho was overexpressed in HK-2 cells. (**A**) mRNA and protein level of Klotho in HK-2 cells with vector or Klotho overexpression. (**B**) Cell viability of HK-2 cells stimulated with H_2O_2. (**C**) Cell proliferation of HK-2 cells stimulated with H_2O_2. (**D**) mRNA levels of fibrosis-related genes in HK-2 cells stimulated with H_2O_2. (**E**) protein levels of fibrosis-related genes in HK-2 cells stimulated with H_2O_2. $^{*}p < 0.05$, $^{**}p < 0.01$, $^{***}p < 0.001$, $^{***}p < 0.0001$.

inhibitor treatment upregulated klotho expression and suppressed fibrotic-related genes (Fig. 4E and F). These findings suggest that ROS may suppress klotho expression through the upregulation of miR-556.

ROS activates Nrf2 to upregulate the expression of miR-556

Nrf2 is a transcription factor activated in response to oxidative stress[22]. We assessed if Nrf2 is involved in the regulation of miR-556 and klotho expression. H_2O_2 treatment promoted nuclear accumulation of Nrf2 in HK-2 cells (Fig. 5A). Knockdown of Nrf2 with shRNA reduced miR-556 while increased klotho expression (Fig. 5B), and suppressed the expression of fibrotic genes (Fig. 5C). In align with this, Nrf2 inhibitor ML385 showed similar effect in inducing klotho, and suppressing miR-556 and fibrotic genes (Fig. 5D and E). These findings emphasize the role of Nrf2 in oxidative stress-induced cellular responses and its involvement in regulating key molecular pathways that impact aging and fibrosis in renal cells. The results provide insights into how targeting the Nrf2-miR-556 axis could be beneficial in managing the deleterious effects of oxidative stress in chronic kidney disease.

Discussion

CKD is characterized by renal fibrosis, a crucial factor leading to irreversible tissue damage and functional decline in the kidneys. Oxidative stress plays a pivotal role in kidney damage by promoting fibrotic processes through various mechanisms. In this study, we discovered that oxidative stress significantly suppresses klotho expression in HK-2 cell, accompanied with the upregulation of fibrosis markers, while ROS scavenger NAC was able to partially restore klotho levels and reduce fibrotic activity, suggesting a therapeutic potential of

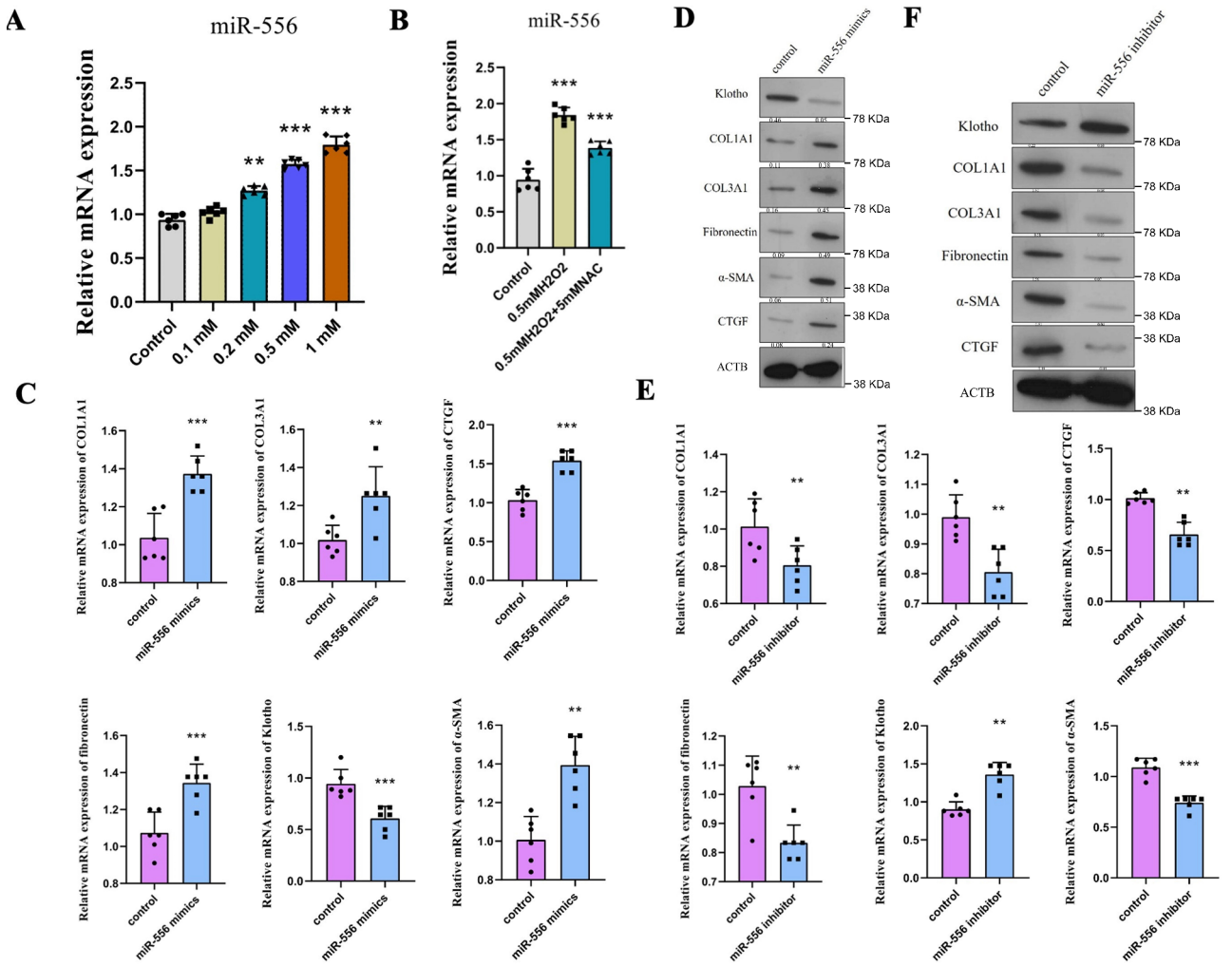

Fig. 4. ROS inhibits Klotho expression by upregulating miR-556. (**A**) expression levels of miR-556 in HK-2 cells stimulated with vehicle control or H_2O_2. (**B**) expression levels of miR-556 in HK-2 cells stimulated with vehicle control or H_2O_2 and NAC. (**C**,**D**) mRNA (**C**) and protein (**D**) levels of fibrotic genes in HK-2 cells with control or miR-556 mimics. (**E**,**F**) mRNA (**E**) and protein (**F**) levels of fibrotic genes in HK-2 cells with control or miR-556 inhibitor. ** $p < 0.01$, *** $p < 0.001$.

antioxidants in renal fibrosis management. Additionally, overexpression of klotho could mitigate the effects of oxidative stress by downregulating fibrosis-associated genes. Our findings further reveal a novel regulatory pathway that oxidative stress-induced Nrf2 activation upregulates miR-556, leading to subsequently suppression of klotho. These insights highlight crucial molecular targets, offering potential strategies for pharmacological or genetic interventions to prevent or manage CKD progression.

ROS play a crucial role in the development and progression of CKD fibrosis. Studies have shown that ROS contribute to sustained cell growth, inflammation, and excessive tissue remodeling, accelerating renal damage[9,23]. ROS-induced oxidative stress leads to the upregulation of fibrosis markers and the activation of profibrogenic pathways, such as the transforming growth factor beta (TGF-β) pathway[9]. Additionally, the Na/K-ATPase/Src complex and NADPH oxidases (NOXs) form an oxidant amplification loop that exacerbates ROS production, contributing to renal fibrosis progression[24]. Furthermore, NOX5 has been identified as a key prooxidant enzyme in diabetic kidney disease, enhancing kidney damage through increased ROS formation and modulation of various signaling pathways involved in fibrosis and inflammation[25]. These findings underscore the significant impact of ROS in driving CKD fibrosis.

Whereas klotho plays a crucial role in CKD fibrosis by exerting anti-fibrotic effects. Studies have shown that klotho deficiency is associated with the progression of CKD stages[26], while klotho supplementation has been found to reverse renal damage, decrease fibrosis index, and reduce the expression of fibrotic markers like collagen I and transforming growth factor β[27]. Additionally, klotho-derived peptides have been identified as potential therapeutic agents that target the TGF-β signaling pathway to inhibit fibroblast activation and ameliorate renal fibrosis[28]. Furthermore,, alpha-klotho protein levels negatively correlated with TGF-β1 in diabetic nephropathy patients, suggesting a role in preventing fibrogenesis and serving as a prognostic marker for disease severity[29].

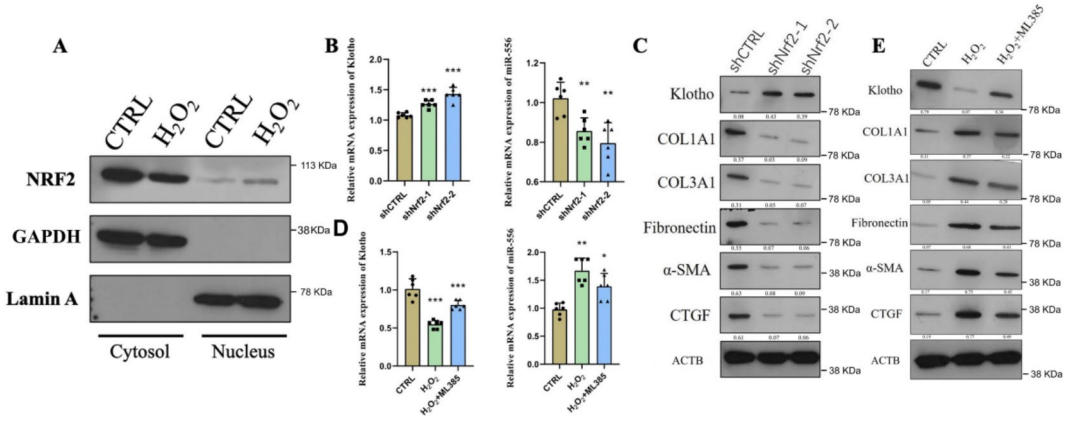

Fig. 5. ROS activates Nrf2 to upregulate the expression of miR-556. (**A**) Nrf2 levels in the cytosol and nucleus fraction of HK-2 cells stimulated with vehicle control or H_2O_2. (**B**) Klotho and miR-556 expression in HK-2 cells with shCTRL or shNrf2. (**C**) Klotho and fibrotic gene expression in HK-2 cells with shCTRL or shNrf2. (**D**) Klotho and miR-556 expression in HK-2 cells with control or Nrf2 inhibitor ML385. (**E**) Klotho and fibrotic gene expression in HK-2 cells with shCTRL or shNrf2. $^{*}p < 0.1$, $^{**}p < 0.01$, $^{***}p < 0.001$.

Overall, klotho emerges as a promising target in combating fibrosis in CKD through its anti-fibrotic properties and regulatory effects on key signaling pathways.

Previous studies reported that oxidative stress responses, wherein the reduction of klotho was accompanied by upregulation of fibrotic markers such as COL1A1, COL3A1, fibronectin, and α-SMA[30,31], while reported that antioxidants could restore klotho levels and inhibit fibrosis[32,33], which are in consistent with our data showing that increasing concentrations of H_2O_2 led to a dose-dependent suppression of klotho. This suppression correlates with an upregulation of fibrosis markers such as COL1A1, COL3A1, fibronectin, and α-SMA. These results strongly suggest that oxidative stress is a pivotal factor in reducing klotho expression, thereby contributing to the fibrotic processes observed in CKD.

Nrf2 is a key regulator of oxidative stress responses and plays a crucial role in CKD fibrosis by regulating oxidative stress, antioxidant pathways, and fibrotic signaling. Nrf2 activation can alleviate oxidative damage and renal fibrosis in CKD[34,35]. Nrf2 activation enhances antioxidant capacity, reduces oxidative stress, and downregulates fibrotic pathways like TGF-β1, ultimately delaying CKD progression[36]. Additionally, Nrf2 activation targets key molecules involved in fibrosis to attenuate tubulointerstitial fibrosis in renal cells[37]. Moreover, Nrf2 activation is associated with mitochondrial homeostasis improvement, further contributing to the mitigation of fibrosis in CKD. Our further analysis demonstrated the role of miR-556-3p as a crucial mediator in this regulatory pathway. We found that oxidative stress, through the activation of the Nrf2 pathway, significantly increases the expression of miR-556-3p. The upregulated miR-556-3p then acts to suppress klotho expression, reinforcing the fibrotic response. This novel finding highlights the intricate molecular interplay where Nrf2, typically known for its protective role against oxidative damage, paradoxically promotes the expression of a miRNA that contributes to detrimental outcomes in kidney cells.

The suppression of klotho by miR-556-3p under oxidative conditions suggests a complex regulatory mechanism that could be manipulated for therapeutic benefit. Prior studies have highlighted Nrf2's role in modulating oxidative stress and inflammation through interactions with various miRNAs, including miR-556 [38,39]. Our investigation revealed that Nrf2 activation leads to the upregulation of miR-556-3p, which subsequently suppresses klotho expression. We further found that suppressing miR-556-3p led to increased klotho expression and reduced expression of fibrosis markers.

With the fast-developing techniques in drug delivery, it becomes feasible to targeting critical mediators in the signaling pathways that contribute to disease progression. Our study elaborated the oxidative stress induced Nrf2-miR-556-3p-klotho pathway also provided several targetable molecules for the treatment of CKD, which could be further evaluated in animal model of CKD. Considering the protective effects of klotho against oxidative stress and fibrosis demonstrated in our study and others, therapies aimed at increasing klotho levels directly, such as gene therapy or klotho protein supplementation, could provide innovative treatments for CKD patients. Previous studies have reported recombinant α-Klotho protein is safe and efficacious, and might be a promising prophylactic or therapeutic option for prevention or retardation of AKI-to-CKD progression[40]. Recent advances in miRNA delivery also facilitated the investigation of therapeutic potentials of small RNAs that targeting genes of interest[41]. By targeting Nrf2 or miR-556-3p and subsequently restore klotho expression, we may be able to offer a new approach to mitigating fibrosis and slowing CKD progression. Considering the central role of oxidative stress in CKD pathogenesis, strategies that enhance the cellular antioxidant responses through Nrf2 could be particularly beneficial. Moreover, the inhibition of miR-556-3p presents another promising avenue. Given our findings that miR-556-3p downregulation leads to an increase in klotho, which is protective against fibrosis, developing miR-556-3p inhibitors could potentially be a direct method to enhance klotho levels and reduce fibrosis. Studies targeting similar miRNAs in other diseases suggest the feasibility of this approach[42].

However, our current study also has certain limitations. Primarily, the use of an in vitro model may not fully replicate the in vivo environment, potentially limiting the generalizability of the findings. Future studies should include in vivo models to validate these results and confirm the therapeutic potential of targeting the Nrf2-miR-556-3p-Klotho pathway. Additionally, the oxidative stress conditions were limited to specific H_2O_2 concentrations, which may not encompass the full spectrum of oxidative stress conditions encountered in vivo. Exploring a broader range of oxidative stress sources and levels in future studies would provide a more comprehensive understanding of these mechanisms. The study also involved short-term exposure to oxidative stress, which may not fully capture the long-term effects of oxidative stress on klotho expression and fibrosis in CKD. Lastly, while this study offers valuable mechanistic insights, clinical data are necessary to support the translational relevance of the findings. Future research should aim to correlate these molecular mechanisms with clinical outcomes in CKD patients.

To confirm and expand upon the findings of this study, several future research directions are suggested. Firstly, in vivo experiments are crucial to validate the in vitro results and to understand the complex interactions in a whole-organism context. Animal models of CKD should be employed to examine the role of the Nrf2-miR-556-3p-Klotho pathway in renal fibrosis and to test the therapeutic potential of modulating this pathway via using antioxidant, or supplementating of klotho.

In conclusion, this study advances the field of renal disease research by providing new insights into the molecular mechanisms of oxidative stress and its impact on renal fibrosis. By identifying the Nrf2-miR-556-3p-Klotho axis as a critical pathway in the regulation of fibrosis, we have highlighted potential therapeutic targets that could be leveraged to develop novel treatments for CKD.

Data availability

All data generated during this study are available from the corresponding author on reasonable request.

Received: 22 September 2024; Accepted: 3 January 2025
Published online: 09 April 2025

References

1. Kovesdy, C. P. Epidemiology of chronic kidney disease: an update 2022. *Kidney Int. Suppl.* **12**, 7–11 (2022).
2. Harambat, J. & Morin, D. Épidémiologie des maladies rénales chroniques en pédiatrie. *Med. Sci. (Paris)* **39**, 209–218 (2023).
3. Garcia Sanchez, J. J. et al. The growing burden of chronic kidney disease in the UK: an impact CKD analysis. *Nephrol. Dial Transpl.* **38**(Suppl 1), gfad063c4271 (2023).
4. Weldetensae, M. K., Weldegebreial, M. G. & Gebreselassie, M. Burden and predictors of chronic kidney disease in developing country. *J. Nephrol. Endocrinol. Res.* 1–7. https://doi.org/10.47363/jone/2022(2)123 (2022).
5. Provenzano, M., Mancuso, C., Garofalo, C., De Nicola, L. & Andreucci, M. Temporal variation of chronic kidney Disease's epidemiology. *G Ital. Nefrol* **36**(2), 2019–vol2 (2019).
6. Nørregaard, R., Mutsaers, H. M., Frøkiær, J. & Kwon, T. H. Obstructive nephropathy and molecular pathophysiology of renal interstitial fibrosis. *Physiol. Rev.* **103**, 2847–2892 (2023).
7. Schroeder, M. Oxidative stress pathways in the pathogenesis of renal fibrosis. Doctoral dissertation, University of Göttingen. University of Göttingen Repository. https://ediss.uni-goettingen.de/handle/11858/00-1735-0000-0028-875B-8 (2015).
8. Saini, V. Academic Press,. The role of oxidative stress in kidney diseases. In *Novel Therapeutic Approaches Targeting Oxidative Stress.* Maurya, P. K. & Qamar, I. (eds) 119–141 (2022).
9. Plöger, H. M. Oxidative stress in the pathogenesis of renal injury: the effect of the antioxidant danshensu on renal fibrosis. https://doi.org/10.53846/goediss-9561 (2022).
10. Okamura, D. M. & Pennathur, S. The balance of powers: Redox regulation of fibrogenic pathways in kidney injury. *Redox Biol.* **6**, 495–504 (2015).
11. Tang, A. et al. Klotho's impact on diabetic nephropathy and its emerging connection to diabetic retinopathy. *Front. Endocrinol.* **14**, (2023).
12. Nakayama, S. et al. Klotho protects chromosomal DNA from radiation-induced damage. *J. Biochem.* **173**, 375–382 (2023).
13. Donate-Correa, J., Martín-Carro, B., Cannata-Andía, J. B., Mora-Fernández, C. & Navarro-González, J. F. Klotho, oxidative stress, and mitochondrial damage in kidney disease. *Antioxidants* **12**, 239 (2023).
14. Jena, S., Sarangi, P., Das, U. K., Lamare, A. A. & Rattan, R. Serum α- Klotho Protein Can Be an Independent Predictive Marker of Oxidative Stress (OS) and Declining Glomerular Function Rate in Chronic Kidney Disease (CKD) Patients. *Cureus*. https://doi.org/10.7759/cureus.25759 (2022).
15. Suzuki, H. I. Roles of MicroRNAs in Disease Biology. *JMA J.* **6**, 104–113 (2023).
16. Phulkerd, T. et al. Circulating and urinary microRNAs profile for predicting renal recovery from severe acute kidney injury. *J. Intensive Care* **10**, 45 (2022).
17. Navarro-Quiroz, E. et al. High-throughput sequencing reveals circulating miRNAs as potential biomarkers of kidney damage in patients with systemic lupus erythematosus. *PLoS One* **11**, e0166202 (2016).
18. Mehi, S. J., Maltare, A., Abraham, C. R. & King, G. D. MicroRNA-339 and microRNA-556 regulate Klotho expression in vitro. *Age (Dordr)* **36**, 141–149 (2014).
19. Feng, C. et al. miRNA-556-3p promotes human bladder cancer proliferation, migration, and invasion by negatively regulating DAB2IP expression. *Int. J. Oncol.* **50**, 2101–2112 (2017).
20. Li, S. S. et al. Upstream and downstream regulators of Klotho expression in chronic kidney disease. *Metabolism* **142**, 155530 (2023).
21. Qiu, J., Liu, X., Yang, G., Gui, Z. & Ding, S. MiR-29b level-mediated regulation of Klotho methylation via DNMT3A targeting in chronic obstructive pulmonary disease. *Cells Dev.* **174**, 203827 (2023).
22. Hammad, M. et al. Roles of oxidative stress and NRF2 signaling in pathogenic and non-pathogenic cells: a possible general mechanism of resistance to therapy. *Antioxidants* **12**, 1371 (2023).
23. Zhao, Y. et al. ROS promote hyper-methylation of NDRG2 promoters in a DNMTS-dependent manner: contributes to the progression of renal fibrosis. *Redox Biol.* **62**, 102674 (2023).
24. Zhang, H., Lai, F., Cheng, X. & Wang, Y. Involvement of NADPH oxidases in the Na/KATPase/Src/ROS oxidant amplification loop in renal fibrosis. *Mol. Med. Rep.* **28** (2023).
25. Jha, J. C. et al. Independent of renox, NOX5 promotes renal inflammation and fibrosis in diabetes by activating ROS-Sensitive pathways. *Diabetes* **71**, 1282–1298 (2022).
26. Martín-Carro, B. et al. Role of Klotho and AGE/RAGE-WNT/B-Catenin signalling pathway on the development of cardiac and renal fibrosis in diabetes. *Int. J. Mol. Sci.* **24**, 5241 (2023).

27. Kim, S. H. et al. Urine-derived stem cell-secreted klotho plays a crucial role in the HK-2 fibrosis model by inhibiting the TGF-B signaling pathway. *Int. J. Mol. Sci.* **23**, 5012 (2022).
28. Yuan, Q. et al. A Klotho-derived peptide protects against kidney fibrosis by targeting TGF-β signaling. *Nat. Commun.* **13**, (2022).
29. INTERNATIONAL JOURNAL OF SCIENTIFIC RESEARCH. *Int. J. Sci. Res.* https://doi.org/10.36106/ijsr. (2019).
30. Chen, D., Tavana, O. & Gu, W. ARF–NRF2: a new checkpoint for oxidative stress responses? *Mol. Cell. Oncol.* **5**, e1432256 (2018).
31. Abdul-Aziz, A., MacEwan, D. J., Bowles, K. M. & Rushworth, S. A. Oxidative stress responses and NRF2 in human leukaemia. *Oxid Med Cell Longev.* **2015**, 1–7 (2015).
32. Wu, A. G. et al. Targeting NRF2-Mediated Oxidative Stress Response in Traumatic Brain Injury: Therapeutic Perspectives of Phytochemicals. *Oxid Med Cell Longev.* **2022**, 1–24. (2022).
33. Li, J. et al. Resveratrol alleviates inflammatory responses and oxidative stress in rat kidney ischemia-reperfusion injury and H2O2-Induced NRK-52E cells via the NRF2/TLR4/NF-KB pathway. *Cell. Physiol. Biochem.* **45**, 1677–1689 (2018).
34. Long, X., Liu, Z., Sun, Y. & Zhang, H. The protective role of NRF2 in renal tubular cells in oxidised Low-Density Lipoprotein-Induced fibrosis. *Anal Cell Pathol (Amst).* **2023**, 1–8. (2023).
35. Qiao, P. et al. Activation of NRF2 signaling pathway delays the progression of hyperuricemic nephropathy by reducing oxidative stress. *Antioxidants* **12**, 1022 (2023).
36. Aihara, S. et al. Spermidine from arginine metabolism activates Nrf2 and inhibits kidney fibrosis. *Commun. Biol.* **6**, (2023).
37. Aranda-Rivera, A. K., Cruz-Gregorio, A., Pedraza-Chaverri, J. & Scholze, A. NRF2 activation in chronic kidney disease: promises and pitfalls. *Antioxidants* **11**, 1112 (2022).
38. Zhao, W. et al. Astrocytic Nrf2 expression protects spinal cord from oxidative stress following spinal cord injury in a male mouse model. *J. Neuroinflammation* **19**, (2022).
39. Mahajan, M. & Sitasawad, S. MIR-140-5P attenuates Hypoxia-Induced breast cancer progression by targeting NRF2/HO-1 axis in a KEAP1-Independent mechanism. *Cells* **11**, 12 (2021).
40. Hu, M. C. et al. Recombinant α-Klotho may be prophylactic and therapeutic for acute to chronic kidney disease progression and uremic cardiomyopathy. *Kidney Int.* **91**, 1104–1114 (2017).
41. Moraes, F. C., Pichon, C., Letourneur, D. & Chaubet, F. miRNA delivery by nanosystems: state of the art and perspectives. *Pharmaceutics* **13**, 1901 (2021).
42. Kim, T. & Croce, C. M. MicroRNA: trends in clinical trials of cancer diagnosis and therapy strategies. *Exp. Mol. Med.* **55**, 1314–1321 (2023).

Author contributions

Study conception and design: DZ; data collection: DZ, ZL, and YG; analysis and interpretation of results: DZ, YG, and HS; draft manuscript preparation: DZ, ZL, and YG. All authors reviewed the results and approved the final version of the manuscript.

Declarations

Competing interests

The authors declare no competing interests.

Additional information

Correspondence and requests for materials should be addressed to D.Z.

Reprints and permissions information is available at www.nature.com/reprints.

Publisher's note Springer Nature remains neutral with regard to jurisdictional claims in published maps and institutional affiliations.